Supporting Information for the Communication

Cycloketyl Radical Mediated Living Polymerization**

Xuefeng Zheng, ‡ Miao Yue, ‡ Peng Yang, Qi Li, Wantai Yang*

College of Materials Science and Engineering, Beijing University of Chemical Technology, Beijing, 100029

*: the corresponding author, E-mail: yangwt@mail.buct.edu.cn

‡These authors contributed equally.

Materials. Tetrahydrofuran (THF) (Beijing Sinopharm Reagent Co., Ltd., 99%), methyl methacrylate (MMA) (Beijing Sinopharm Reagent Co., Ltd., 99%), n-butyl acrylate (BA) (Beijing Sinopharm Reagent Co., Ltd., 99%), methyl acrylate (MA) (Beijing Sinopharm Reagent Co., Ltd., 99%), glycidyl methacrylate (GMA) (Beijing Sinopharm Reagent Co., Ltd., 99%) and styrene (St) (Beijing Sinopharm Reagent Co., Ltd., 99%) were passed through a column filled with basic alumina, dried over calcium hydride, and distilled under reduced pressure. Zn (Alfa, 99%), xanthone (Alfa, 99%), NH_4Cl (Beijing Sinopharm Reagent Co., Ltd., 99%), and methanol(Beijing Sinopharm Reagent Co., Ltd., 99%) were used as received.

Synthesis of 9, 9'-bixanthene-9, 9'-diol (BIXANDL). Zn powder (4mmol, 0.26g) and xanthone (2mmol) were mixed in a solution containing 3 cm^3 saturated aqueous NH_4Cl and 5cm^3 THF. The mixture was stirred at room temperature. The temperature rose, and after 10min the Zn powder disappeared. The solvents were then evaporated to dryness, and the product was extracted with diethyl ether. The ether layer was separated and evaporated to dryness to afford the pure compound BIXANDL. ^{1}H NMR ($CDCl_3$): δ 6.82 (d, 4H), 6.96 (t, 4H), 7.09 (d, 4H), 7.26 (t, 4H). The hydrogen structure in BIXANDL corresponding to every chemical shift is indicated in Chart S1. ^{1}H NMR data of the compound by using $CDCl_3$ as solvent in our work (6.82, d, 4H; 6.96, t, 4H; 7.09, d, 4H; 7.26, t, 4H) is close to the reported value in the original report by using $(CD_3)_2CO$ as solvent (6.85, d, 4H; 7.00, t, 4H; 7.29, d, 4H; 7.31, t, 4H).[1] Instead the use of chloroform as the solvent in our paper, the use of the solvent acetone in the original report leads that the two types of hydrogen structures at 7.29 and 7.31 ppm in the original report shift to 7.09 and 7.26 ppm in our work. ^{13}C NMR (Chart S2): 152.5, 129, 127.5, 123, 122, 115, 76. The carbon structure in BIXANDL corresponding to every chemical shift is indicated in Chart S2. Elemental analysis: calculated, C 79.19%, O 16.24%, H 4.57%; found, C 79.12%, O 16.36%, H 4.52%. Mass spectra ($M+H^+$): calculated 394; found 197. This is exactly as same as the observed mass spectra in the original report,[1] because BIXANDL is dissociated to form xanthone monomer under laser irradiation during laser desorption process in mass spectra measurement.

Chart S1. Four kinds of C-H structures in BIXANDL that present four kinds of chemical shift in ^{1}H NMR spectra of BIXANDL (Figure S1) respectively: 7.26 (b, triplet, 4H), 7.09 (a, doublet, 4H), 6.96 (c, triplet, 4H) and 6.82 (d, doublet, 4H).

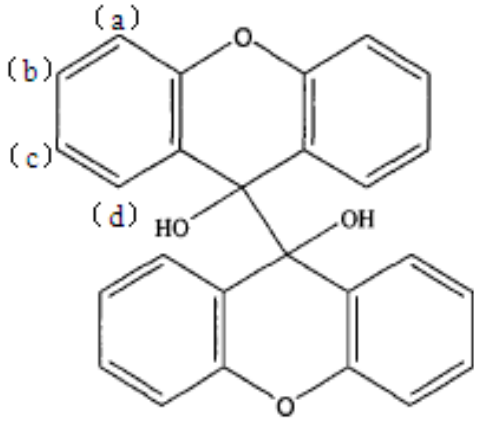

Chart S2. Seven kinds of carbon structures in BIXANDL that present seven kinds of chemical shift in ^{13}C NMR spectra of BIXANDL respectively: 152.5 (1), 129 (4), 127.5 (3), 123 (2), 122 (5), 115 (6), 76 (7).

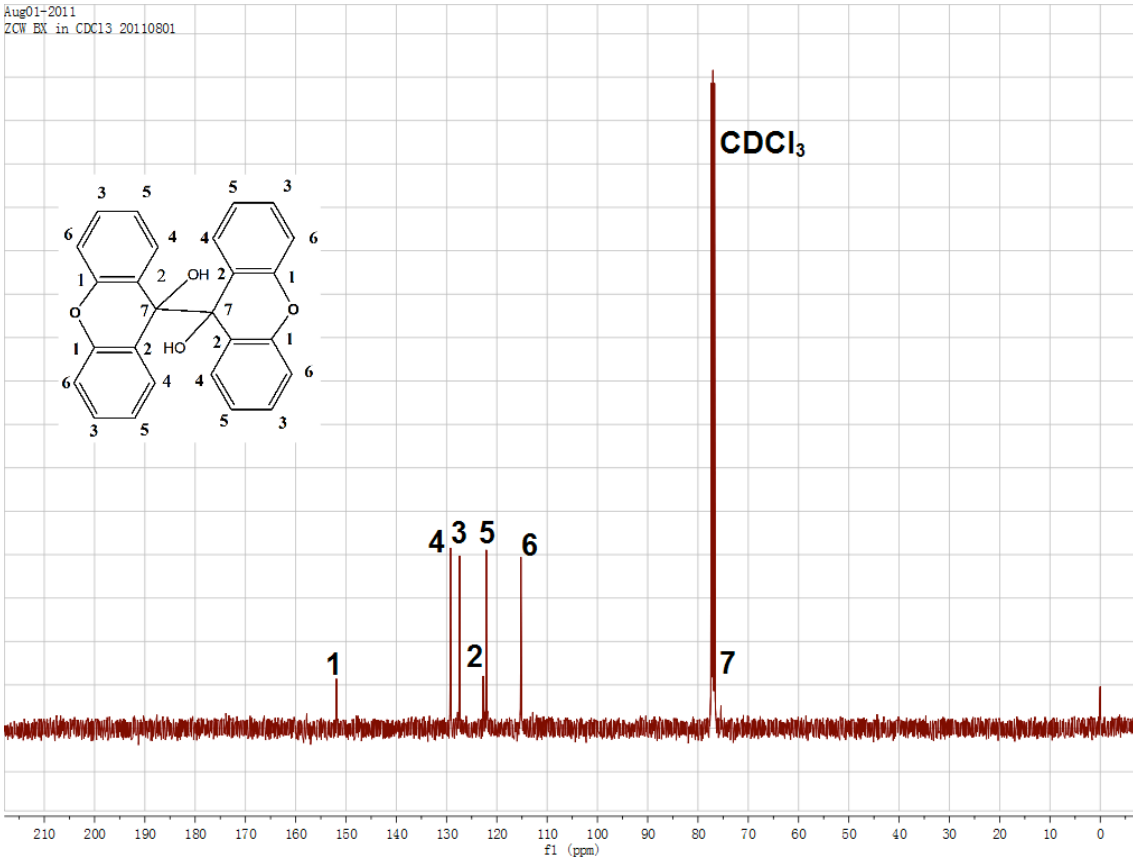

Characterizations. Conversion of monomer was determined by gravimetry at RT. Number and weight average molecular weight (M_n and M_w, respectively) and polydispersity (PDI=M_w/M_n) were determined by gel permeation chromatography (GPC). The GPC was conducted with a Waters 515 pump and Waters 410 differential refractometer using PSS columns (Styrogel 10^5,10^3,10^2 A) in THF as an eluent at 30 °C at a flow rate of 1 mL/min. The column system was calibrated with linear PSt standards. NMR (Bruker AC-600) spectra was recoded in $CDCl_3$ as solvent and was reported in parts million (δ) from internal TMS (for proton). The UV spectroscopy was determined by UV-visible spectrophotometer (Australia,GBC Cintra-20 spectro-photometer), the scan wavelength range was 200-900nm, scanning frequency was 1000nm/min and spectral resolution was 0.427nm.

Bulk polymerization of MMA by thermal-CMP. A solution of MMA and BIXANDL was added into a flask and then the flask was degassed and backfilled with nitrogen (N_2) by three freeze-pump-thaw cycles. Subsequently, the solution was stirred at 70℃ for 4h under nitrogen atmosphere in a glovebox. Samples were taken periodically under N_2 using an N_2-purged syringe, diluted by THF to a known concentration. Polymerization was stopped by quenching in ice-water solution. The resulting mixture was poured into a vigorously stirred methanol (300 mL). The precipitated polymer was collected and dried under vacuum at room temperature (RT).

Typical experimental procedures for the solution polymerization of MMA by thermal-CMP. A solution of MMA, THF and BIXANDL was added into a flask and then the flask was degassed and backfilled with N_2 by three freeze-pump-thaw cycles. Subsequently, the solution was stirred at 70℃ for 12h under nitrogen atmosphere in a glovebox. Samples were taken periodically under N_2 using an N_2-purged syringe, diluted by THF to a known concentration. Polymerization was stopped by quenching in ice-water solution. The resulting mixture was poured into a vigorously stirred methanol (300 mL). The precipitated polymer was collected and dried under vacuum at RT.

Typical experimental procedures for the solution polymerization of St by thermal-CMP. A solution of styrene, THF and BIXANDL was added into a flask and then the flask was degassed and backfilled with N_2 by three freeze-pump-thaw cycles. Subsequently, the solution was stirred at 70℃ for 22h under nitrogen atmosphere in a glovebox. Samples were taken periodically under N_2 using an N_2-purged syringe, diluted by THF to a known concentration. Polymerization was stopped by quenching in ice-water solution. The resulting mixture was poured into a vigorously stirred methanol (300 mL). The precipitated polymer was collected and dried under vacuum at RT.

Synthesis of macroinitiator. A solution of MMA, THF and BIXANDL was added into a flask and then the flask was degassed and backfilled with N_2 by three freeze-pump-thaw cycles. Subsequently, the solution was stirred at 70℃ for certain time under nitrogen atmosphere in a glovebox. Polymerization was stopped by quenching in ice-water solution. The resulting mixture was purred into a vigorously stirred methanol (300 mL). The precipitated polymer was collected and dried under vacuum at RT.

Chain extension by thermal-CMP. A solution of MMA and presynthesized PMMA with cycloketyl xanthone ends (PMMA-CX) (M_n=8500, PDI=1.29) was added into a flask and then the flask was degassed and backfilled with N_2 by three freeze-pump-thaw cycles. Subsequently, the solution was stirred at 70℃ for under nitrogen atmosphere in a glovebox. Samples were taken periodically under N_2 using an N_2-purged syringe, diluted by THF to a known concentration. Polymerization was stopped by quenching in ice-water solution. The resulting mixture was poured into a vigorously stirred methanol (300 mL). The precipitated polymer was collected and dried under vacuum at RT.

Synthesis of Poly(MMA-b-BA) copolymer by thermal-CMP. A solution of BA and PMMA-CX (M_n=35500, PDI=1.46) was added into a flask and then the flask was degassed and backfilled with N_2 by three freeze-pump-thaw cycles. Subsequently, the solution was stirred at 70℃ under nitrogen atmosphere in a glovebox. Samples were taken periodically under N_2 using an N_2-purged syringe, diluted by THF to a known concentration. Polymerization was stopped by quenching in ice-water solution. The resulting mixture was poured into a vigorously stirred methanol (300 mL). The precipitated polymer was collected and dried under vacuum at RT.

Typical experimental procedures for solution polymerization of MMA by photo-CMP. A mixture of MMA, THF and BIXANDL was added to the Pyrex tube and degassed by three freeze-pump-thaw cycles. The tube was subjected to the UV irradiation by a Hitachi UV lamp (VWH) equipped with a high pressure mercury lamp and a U-370 filter which transmits UV within a range of 220 nm < λ < 375 nm. The distance between the reaction tube and the light source was kept at 20 cm. Samples were taken periodically under N_2 atmosphere. After the polymerization, the resulting mixture was poured into a vigorously stirred methanol (300 mL). The precipitated polymer was collected and dried under vacuum at RT. During photo-CMP, vigorous stirring in the samples is always needed to ensure the effect from the retardation of photo intensity across the solution layer on the polymerization could be disregarded.

Chain extension by photo-CMP. A mixture of MMA and PMMA-CX (M_n=42500, PDI=1.59) was added to the Pyrex tube and degassed by three freeze-pump-thaw cycles. The tube was subjected to the UV irradiation by a Hitachi UV lamp (VWH) equipped with a high pressure mercury lamp and a U-370 filter which transmits UV within a range of 220 nm < λ < 375 nm. The distance between the reaction tube and the light source was kept at 20 cm. Samples were taken periodically under N_2 atmosphere. Polymerization was stopped by turning off the light. The resulting mixture was poured into a vigorously stirred methanol (300 mL). The precipitated polymer was collected and dried under vacuum at RT. During photo-CMP, vigorous stirring in the samples is always needed to ensure the effect from the retardation of photo intensity across the solution layer on the polymerization could be disregarded.

Synthesis of Poly(MMA-b-BA) copolymer by photo-CMP. A mixture of BA and PMMA-CX (M_n=61500, PDI=1.68) was added to the Pyrex tube and degassed by three freeze-pump-thaw cycles. The tube was subjected to the UV irradiation by a Hitachi UV lamp (VWH) equipped with a high pressure mercury lamp and a U-370 filter which transmits UV within a range of 220 nm < λ < 375 nm. The distance between the reaction tube and the light

source was kept at 20 cm. Samples were taken periodically under N_2 atmosphere. Polymerization was stopped by turning off the light. The resulting mixture was poured into a vigorously stirred methanol (300 mL). The precipitated polymer was collected and dried under vacuum at RT. During photo-CMP, vigorous stirring in the samples is always needed to ensure the effect from the retardation of photo intensity across the solution layer on the polymerization could be disregarded.

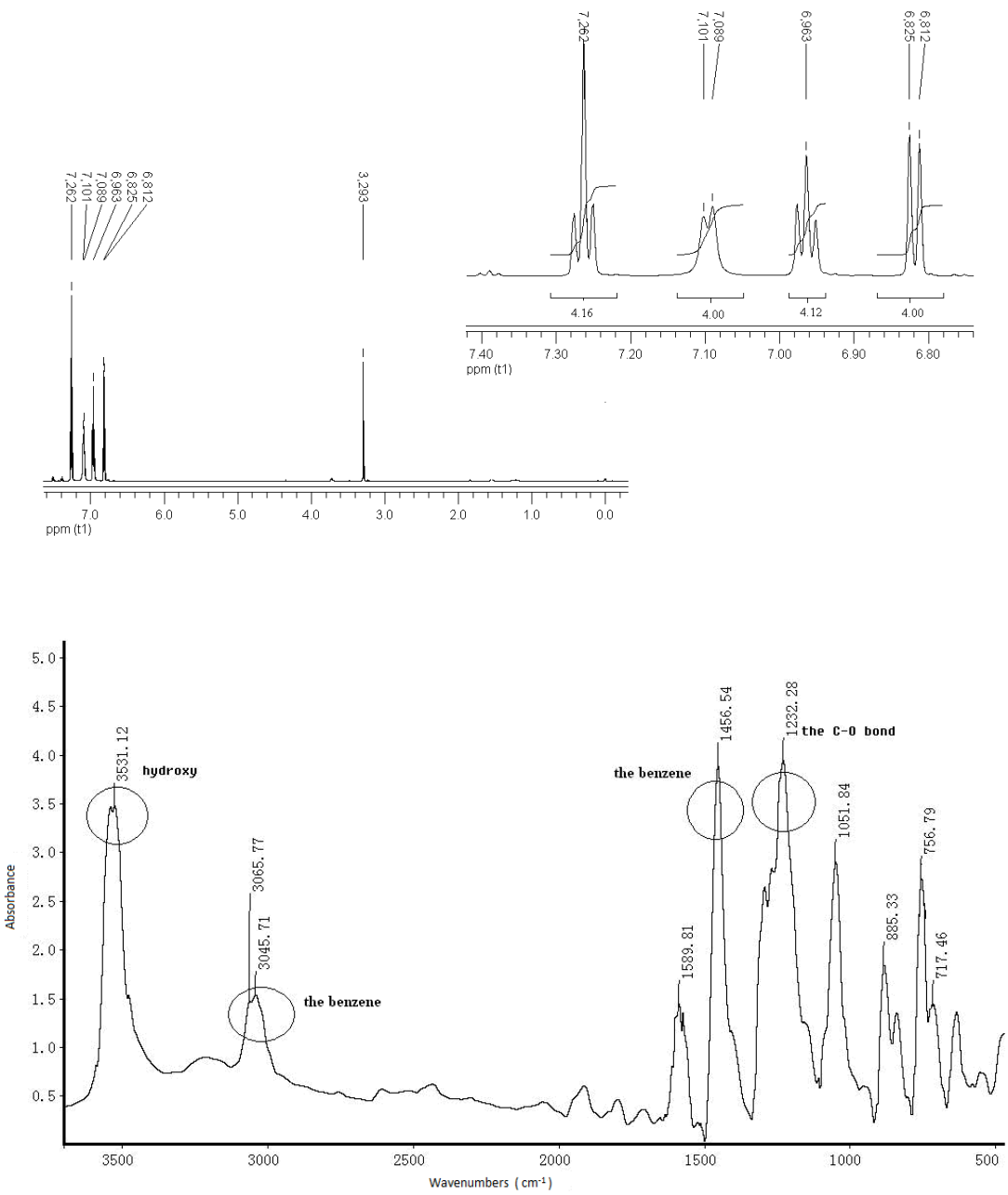

Figure S1. ^{1}H NMR (upper) and FTIR (lower) spectra of synthesized BIXANDL. In the upper figure for NMR, the ratio of four kinds of proton structures is 4.16 (7.26ppm): 4.00 (7.09ppm): 4.12(6.96ppm): 4.00(6.82ppm) that is close to the theoretical value, 4: 4: 4: 4 in BIXANDL compound. The area 4.16 at 7.26 ppm is the net value after subtracting from the background solvent ($CDCl_3$) shift. In the lower figure for FTIR, the characteristic band for carbonyl of xanthone monomer at 1870-1650cm^{-1} is not apparent, indicating the formation of dimer as BIXANDL.

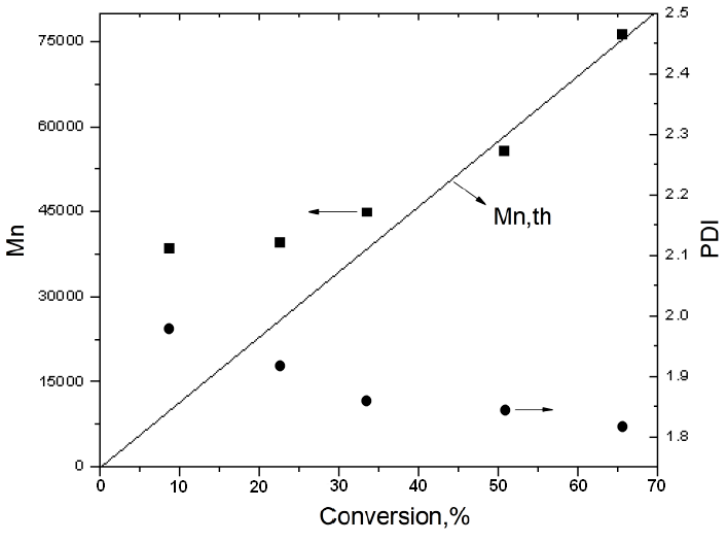

Figure S2. The relationship of M_n and conversion of bulk thermo-CMP of MMA at 70℃ by using 0.3% BIXANDL.

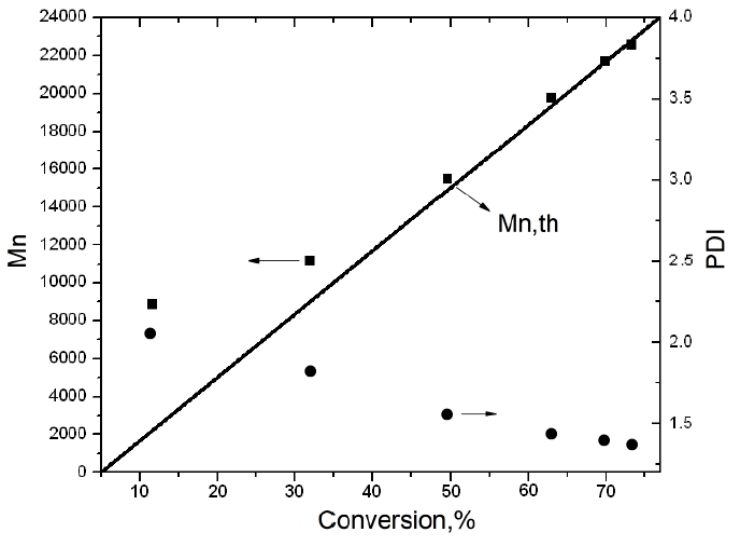

Figure S3. The relationship of M_n and conversion of thermal-CMP of 50% (wt) MMA in THF at 70℃ by using 0.6 % BIXANDL.

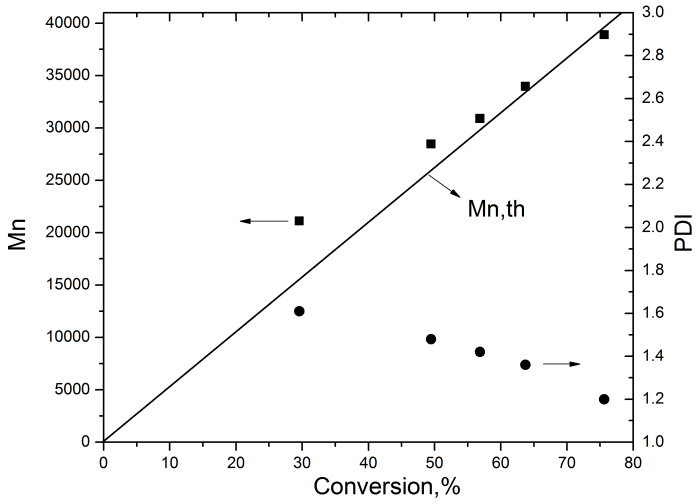

Figure S4. The relationship of M_n and conversion of thermal-CMP of 48% (wt) MMA in acetone at 70℃ by using 0.4 % BIXANDL.

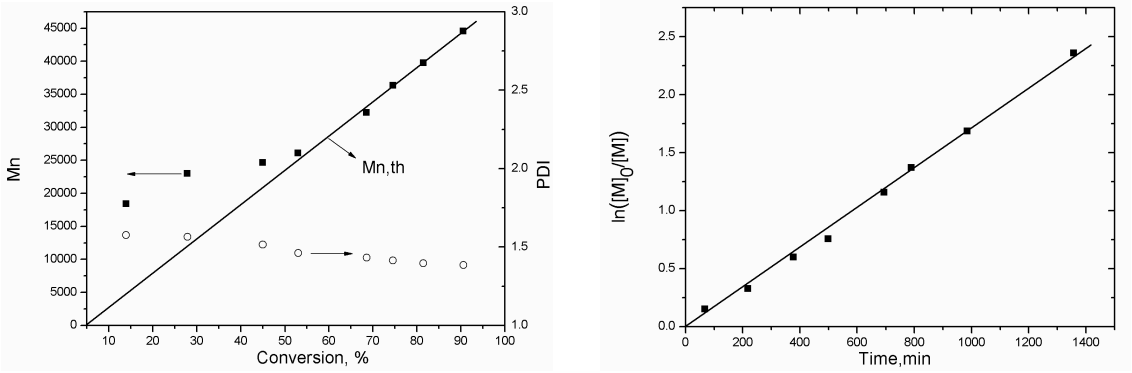

Figure S5. The relationship of M_n and conversion of thermal-CMP of 50% (wt) St in THF at 70℃ by using BIXANDL (0.4% wt).

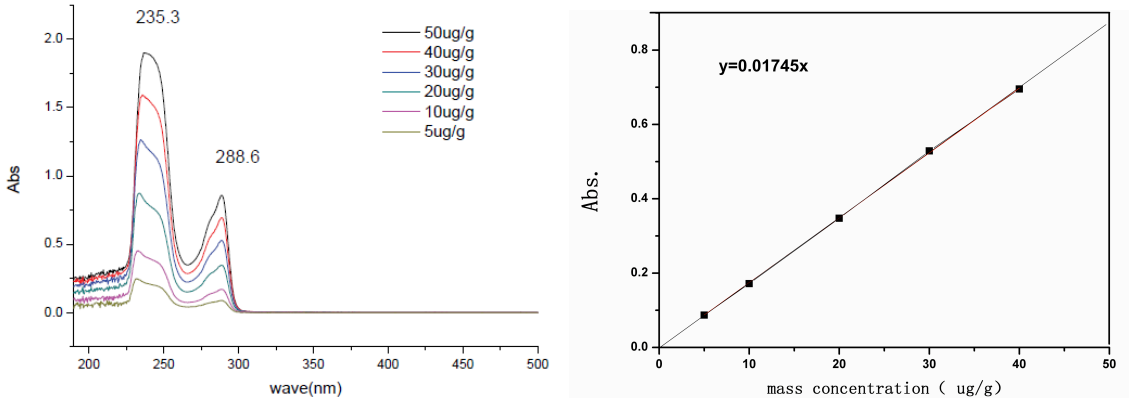

Figure S6. The UV-vis absorption of BIXANDL with different concentration (μg/g) in THF (left) and standard curve (right) with different concentration (μg/g) of BIXANDL in THF (right). The characteristic absorption peaks for BIXANDL in THF are located at 235 and 288 nm. The absorption value at 288 nm is used in the standard curve. In order to calculate the number of CX groups in each polymer chain, the absorption value of the synthesized polymer at 288 nm in UV-vis spectrum was firstly measured. Then after correlating this value into the standard curve, we can obtain the concentration of BIXANDL in each polymer chain as around 1 BIXANDL per chain, which means one chain has two CX groups.

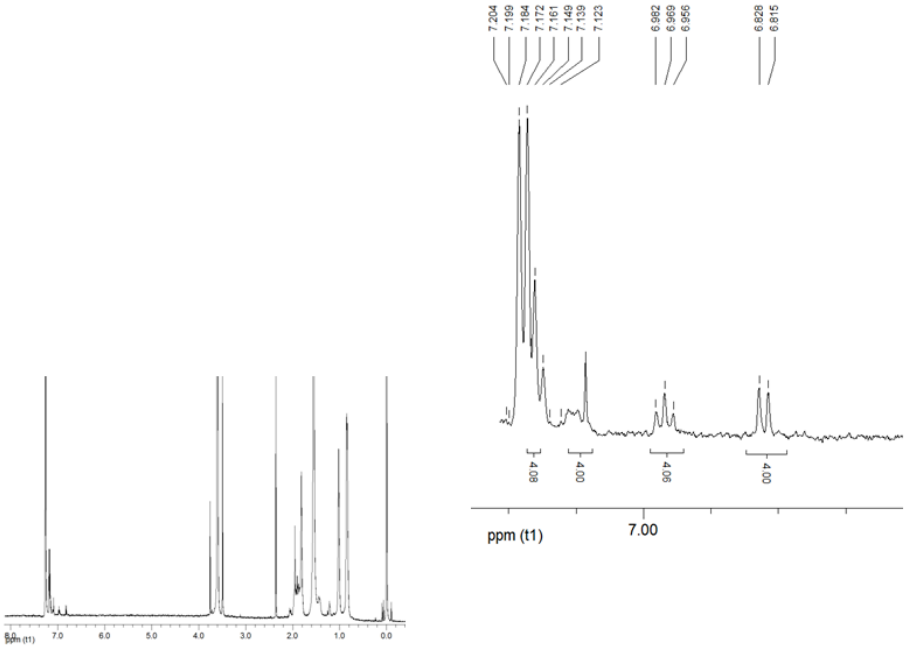

Figure S7. ^{1}H NMR spectrum of PMMA polymer with cycloketyl xanthone structure (CX) as terminal group. Polymerization conditions: bulk CMP polymerization of MMA at 75℃. The chemical shifts at δ =6.82, 6.96, 7.17, 7.26 ppm are assigned to the living terminus of PMMA chain. The shift at 7.26 ppm includes the contribution from solvent CDCl3, and the net ratio of four chemical shifts (6.82, 6.96, 7.17, 7.26) after subtracting from background contribution of $CDCl_3$ at 7.26 ppm is 4.00: 4.05: 4.00: 4.08, which is labeled in the up right insert image.

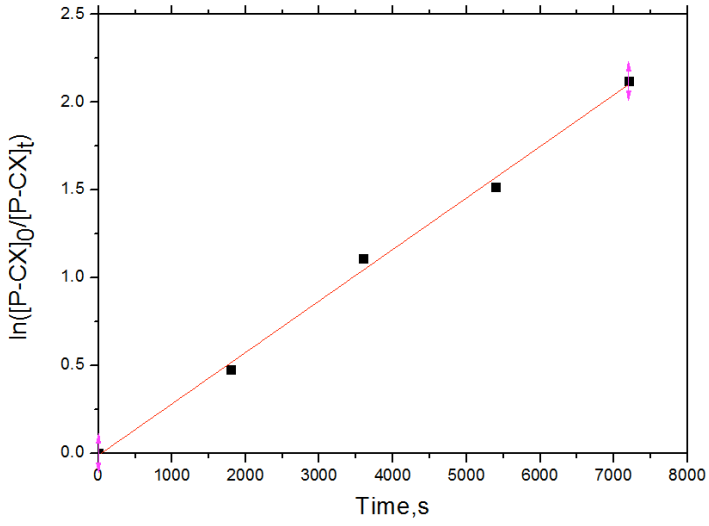

Figure S8. The change of cycloketyl xanthone structure (CX) concentration in PMMA-CX macroinitiator (M_n=10500，PDI= 1.39) sample after incubating in THF solution of TEMPO at 70℃ for different time. The slope of the obtained straight line is the activation rate constant k_a (2.93E-4 s^{-1}), based on the calculations shown in the Appendix 1. The CX concentration was determined by ^{1}H NMR spectroscopy.

Chart S3. The synthesized BIXANDL derivatives with substituted urethane groups on hydroxyl position by the reaction between hydroxyl and ethyl isocyanate: BXD (left) with double substitutions on hydroxyl position and BXS (right) with single substitutions on hydroxyl position.

NMR data for BXD: ^{1}H NMR (600 M, $CDCl_3$): δ (ppm) = 1.05 (6H, $NHCH_2C\boldsymbol{H_3}$), 3.04 (4H, $NHC\boldsymbol{H_2}CH_3$), 4.79 (2H, $N\boldsymbol{H}CH_2CH_3$), 6.70-7.05 (16H, $C_6\boldsymbol{H_4}$).

NMR data for BXS: ^{1}H NMR (600 M, $CDCl_3$): δ (ppm) = 1.05 (3H, $NHCH_2C\boldsymbol{H_3}$), 2.88 (1H, $CO\boldsymbol{H}$), 3.04 (2H, $NHC\boldsymbol{H_2}CH_3$), 4.83 (1H, $N\boldsymbol{H}CH_2CH_3$), 6.78-7.30 (16H, $C_6\boldsymbol{H_4}$).

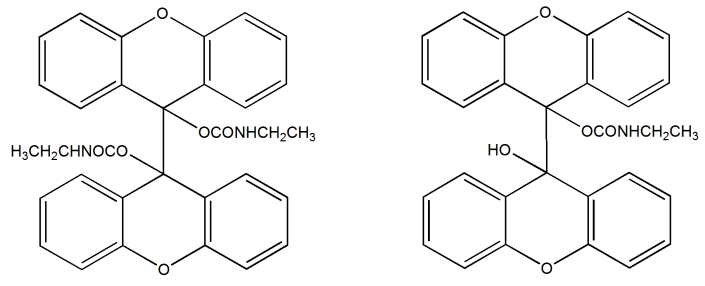

BXD BXS

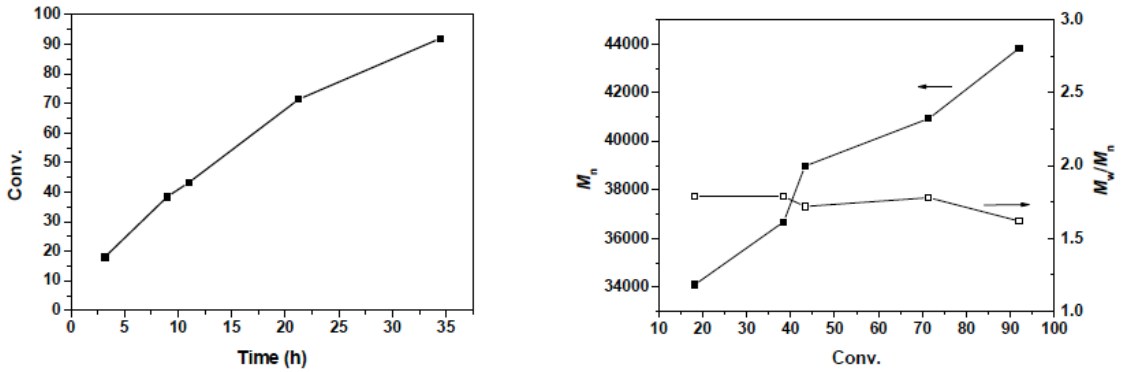

Figure S9. The kinetics curves for the thermal-CMP of MMA at 100℃ in toluene by using BXD to mediate the polymerization. The molar ratio of monomer to BXD is 500:1, the concentration of MMA in toluene is 40 wt%. The designed theoretical molecular weight of polymer product at full conversion is 50000.

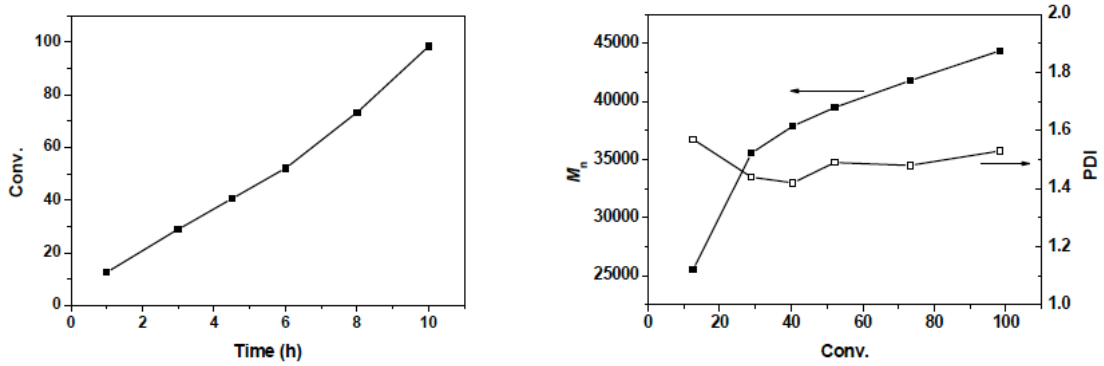

Figure S10. The kinetics curves for the thermal-CMP of MMA at 100℃ in dioxane by using BXS to mediate the polymerization. The molar ratio of monomer to BXD is 500:1, the concentration of MMA in toluene is 50 wt%. The designed theoretical molecular weight of polymer product at full conversion is 50000.

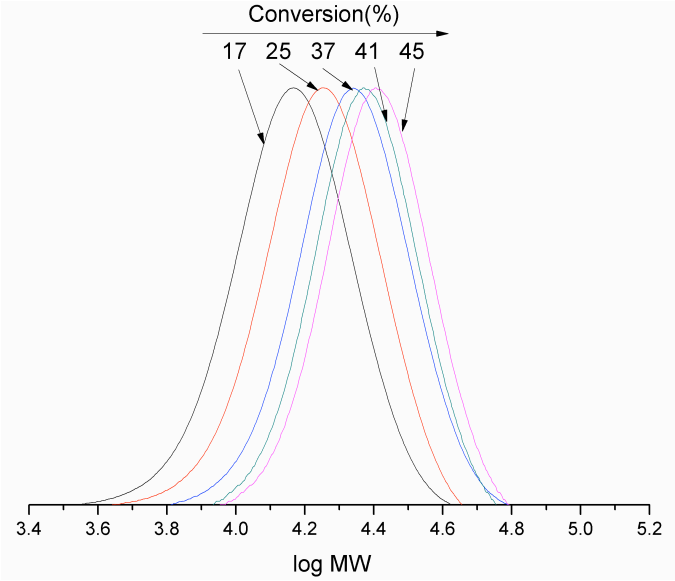

Figure S11. The shift of GPC curve after chain extension by using PMMA-CX (0.7181g) (M_n=8500, PDI=1.29) as macroinitiator to re-initiate the thermal-CMP of MMA (3.1258g) at 70℃ in toluene (5.1354g).

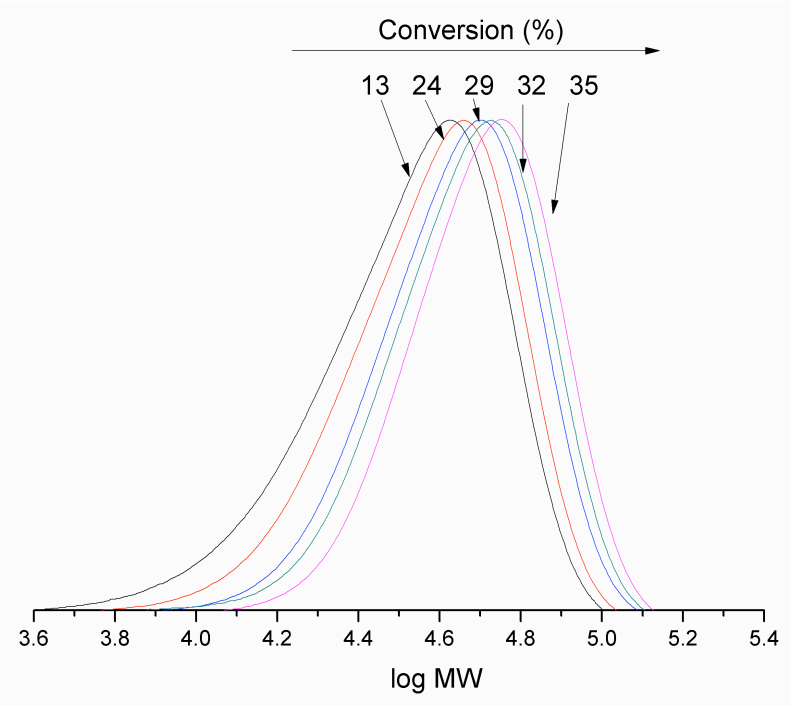

Figure S12. The shift of GPC curve after copolymerization with BA (2.0134g) by using PMMA-CX (1.3745g) (M_n=35500, PDI=1.46) as macroinitiator to re-initiate the thermal-CMP of BA at 70℃ in toluene (5.3128g).

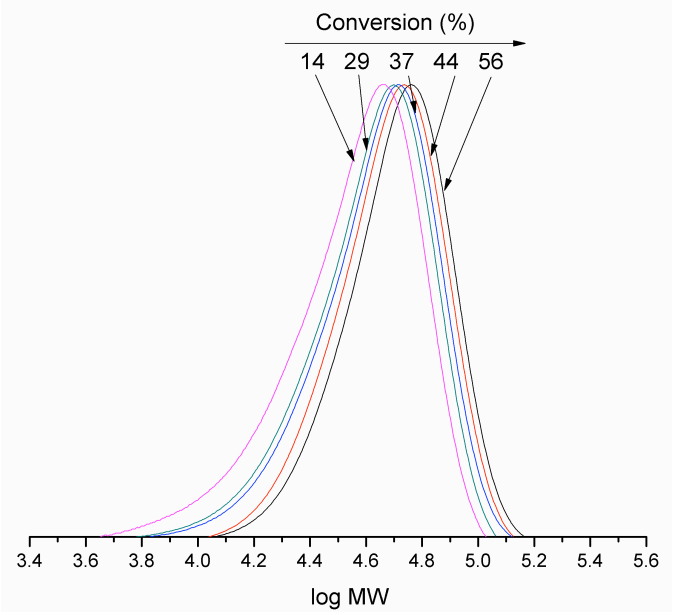

Figure S13. The shift of GPC curve after chain extension by using PMMA-CX (3.3661g) (M_n=42500, PDI=1.59) as macroinitiator to re-initiate the photo-CMP of MMA (2.0123g) at room temperature in toluene (5.1036g). The UV intensity is 3mW/cm^2.

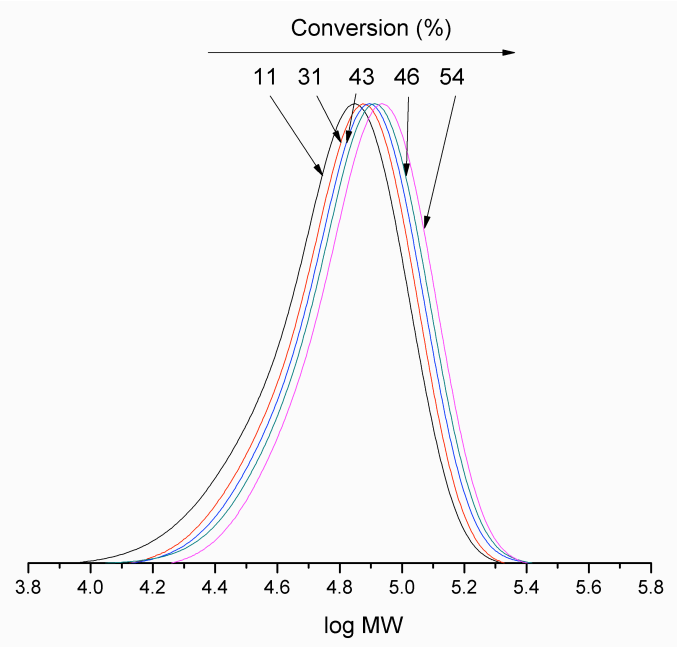

Figure S14. The shift of GPC curve after copolymerization with BA(1.9853g) by using PMMA-CX(3.1474g) (M_n=61500, PDI=1.68) as macroinitiator to re-initiate the photo-CMP of BA at room temperature in toluene (5.0147g) . The UV intensity is 3mW/cm^2.

References

1. M. Takacs, P. Kertesz, G. Toth, J. H. Vajda, *Arch. Pharm*. 1976, **309**, 735.

Appendix 1. The calculation of k_a (c.f. Figure S8).

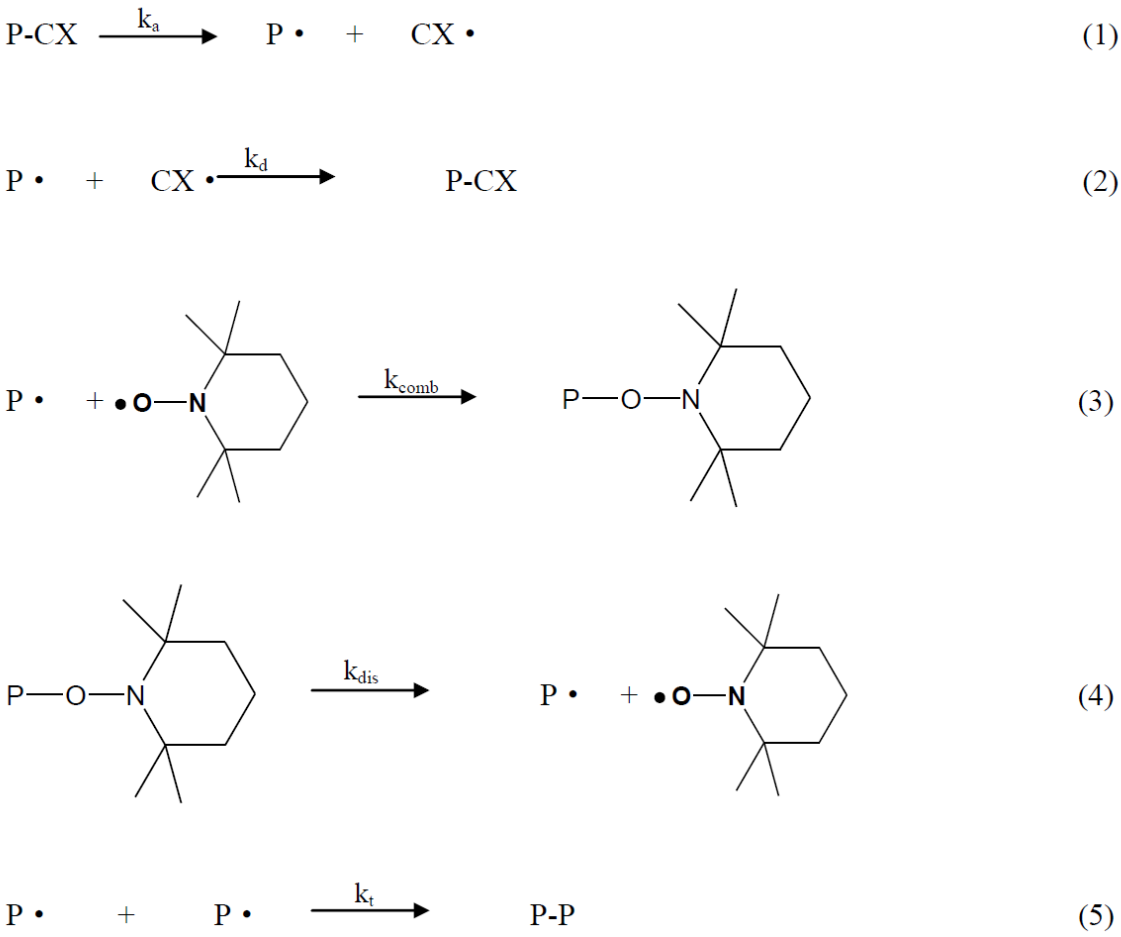

The increasing rate for the concentration of the macroinitiator radical [$P\bullet$] is:

$$\frac{d[P\bullet]}{dt} = k_{act}[P-CX] - k_{deact}[P\bullet][CX\bullet] - k_{comb}[P\bullet][TEMPO\bullet] - 2k_t[P\bullet]^2 + k_{dis}[P-TEMPO] \quad (6)$$

Firstly, because the amount of TEMPO radical [$TEMPO\bullet$] is more access than [$P-CX$], the forming radical species $P\bullet$ and $CX\bullet$ would be quickly quenched by TEMPO, resulting in a fact that [$P\bullet$] and [$CX\bullet$]<< [$TEMPO\bullet$]. Therefore, comparing with $-k_{comb}[P\bullet][TEMPO\bullet]$, $-k_{deact}[P\bullet][CX\bullet]$ and $-2k_t[P\bullet]^2$ could be disregarded.

Secondly, the reaction temperature for performing the experiment in Figure S8 is 70℃. Under such a low temperature, the dissociation rate (k_{dis}) for the adduct with TEMPO ($P-TEMPO$) in reaction (4) is very low, resulting in a fact that k_{dis} << k_{act}, so $k_{dis}[P-TEMPO]$ could be also disregarded. Therefore, the equation (6) is transformed to (7):

$$\frac{d[P\bullet]}{dt} = k_a[P-CX] - k_{comb}[P\bullet][TEMPO\bullet] \quad (7)$$

The decreasing rate for the concentration of the macroinitiator is:

$$\frac{d[P-CX]}{dt} = -k_a[P-CX] + k_d[P\bullet][CX\bullet] \quad (8)$$

Combining (6) with (8), we obtain (9):

$$\frac{d[P\bullet]}{dt} + \frac{d[P-CX]}{dt} = -k_{comb}[P\bullet][TEMPO\bullet] - 2k_t[P\bullet]^2 + k_{dis}[P-TEMPO] \quad (9)$$

disregarding $-2k_t[P\bullet]^2$ and $k_{dis}[P-TEMPO]$, we obtain (10):

$$\frac{d[P\bullet]}{dt} + \frac{d[P-CX]}{dt} = -k_{comb}[P\bullet][TEMPO\bullet] \quad (10)$$

Combining (7) and (10), we obtain (11):

$$-\frac{d[P-CX]}{dt} = k_a[P-CX] \quad (11)$$

Transforming (11) to: $-\frac{d[P-CX]}{[P-CX]} = k_a dt$ (12)

And then transform (12) to integration equation:

$$\ln\frac{[P-CX]_0}{[P-CX]_t} = k_a t \quad (13)$$

Plotting the above equation (13) by using $\ln\frac{[P-CX]_0}{[P-CX]_t}$ as y axis and t as x axis, and Figure S8 could be obtained. The straight slope of the line was k_a.

Appendix 2. The kinetic analysis based on Scheme 1.

Scheme 1. The schematic reaction process of CMP.

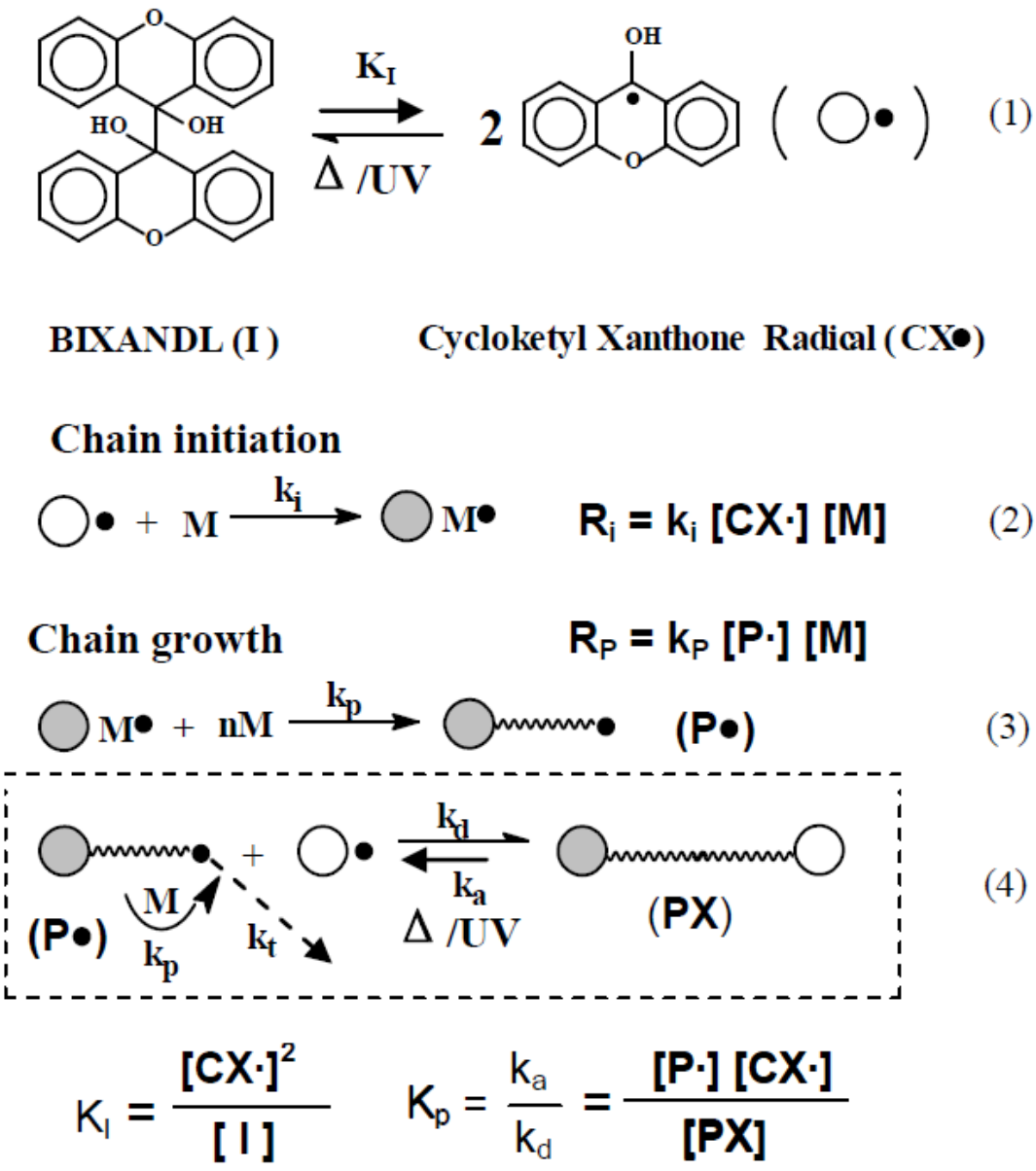

By reaction 4, we obtain

$$[PX] = \frac{k_d[P\bullet][CX\bullet]}{1+k_a} \approx k_d[P\bullet][CX\bullet] \quad \text{since} \quad k_a \text{ as 2.93E-4 } S^{-1} \text{ is } <<1, \qquad (1)$$

By the differential of equation (1), we obtain,

$$\frac{d[PX]}{dt} = k_d[CX\bullet]\frac{d[P\bullet]}{dt} \qquad (2)$$

Substituting the equation $R_i = \frac{d[P\bullet]}{dt} = k_i[CX\bullet][M]$ (c.f. the corresponding analysis in page 3 of the manuscript) into the equation (2), we obtain,

$$\frac{d[PX]}{dt} = k_d[CX\bullet]k_i[CX\bullet][M] = k_d[CX\bullet]^2 k_i[M] \qquad (3)$$

Correlating $K_I = \frac{[CX\bullet]^2}{[I]}$ (at the early stage of the polymerization) with the equation (3), we obtain,

$$\frac{d[PX]}{dt} = k_d[CX\bullet]k_i[CX\bullet][M] = k_d[CX\bullet]^2 k_i[M] = k_i[M]k_d K_I[I] \qquad (4)$$

Combining $[PX] = [I]_0 - [I]$ with the equation (4), followed by the integration, we finally obtain

$$[PX] = [I]_0\left(1 - e^{-Kt}\right) \text{ where } K = k_i[M]k_d K_I \qquad (5)$$

Combining $M_n = \frac{M_m[C]}{[PX]}$ and $M_{n,th} = \frac{M_m[C]}{[I]_0}$ (where M_m is the molecular mass of the monomer, and $[C]$ is the concentration of the polymerized monomers that equal to the multiplication of the starting concentration of the monomer with the conversion of the monomer) with the equation (5), we obtain,

$$\frac{M_n}{M_{n,th}} = \frac{e^{Kt}}{e^{Kt}-1}$$

The schematic curves based on the above equations are shown in the following Figure, and these plots are in well accordance with the experimental results.

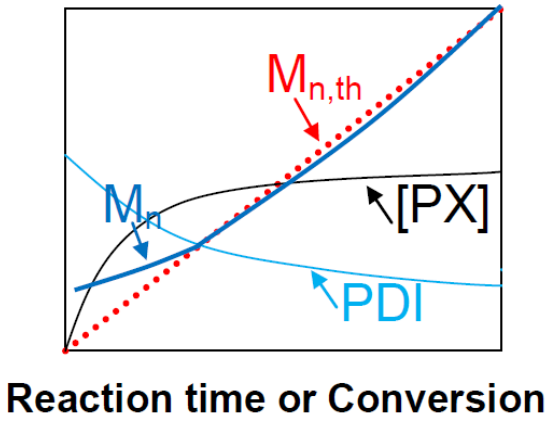

Changing tendency of PDI

Fukuda et al (A. Goto, T. Fukuda, Macromolecules 1997, 30, 4272) proposed an equation about PDI (as follows) where an important parameter y_n, was defined as the average number of activation-deactivation cycles that an adduct experiences during time t, and the smaller y_n, the bigger PDI. For our system, the [P·] in reaction 4 was very low at the beginning of the polymerization while $[CX\cdot]_I$ was high at the same time. Therefore at the beginning of the polymerization, the deactivation reaction R_d would be over the activation reaction R_a so that the y_n was small to result in a high PDI value; then, along with gradual increasing of [P·], a dynamic exchange equilibrium was gradually created, and eventually, elevated y_n values induced a descending PDI. The changing tendency of PDI is schematically, then, drawn manually based on the following equation from Fukuda's theory.

$$M_w/M_n = x_w/x_n = 1 + (2/y_n) + (1/x_n)$$